

## Comparative clinical pharmacology of [ $^{111}\text{In}$ ]-labeled murine monoclonal antibodies

M. G. Rosenblum, J. L. Murray, L. Lamki, G. David, and D. Carlo

<sup>1</sup> Departments of Clinical Immunology and Biological Therapy and of Nuclear Medicine, The University of Texas System Cancer, M. D. Anderson Hospital and Tumor Institute, 1515 Holcombe Drive, Houston, TX 77030, USA

<sup>2</sup> Hybritech Incorporated, San Diego, CA 92121, USA

**Summary.** Patients with metastatic melanoma received either the murine antimelanoma antibody ZME-018 (20 patients) or antibody 96.5 (26 patients) at doses ranging from 1 to 20 mg and coupled to 2.5 or 5 mCi of [ $^{111}\text{In}$ ]. The pharmacokinetics and tissue disposition of these antibodies were measured at various times after infusion of the radiolabel. The clearance of the [ $^{111}\text{In}$ ] label from plasma closely fit ( $r^2 > 0.90$ ) an open, one-compartment mathematical model after administration of antibody 96.5. Clearance of [ $^{111}\text{In}$ ] from plasma after administration of ZME-018 fit a one-compartment model in some patients and a two-compartment model in others. The terminal phase half-lives of 96.5 and ZME-018 antibodies at the 20-mg dose were almost identical ( $27 \pm 2$  h and  $29 \pm 5$  h, respectively). The half-lives calculated for 96.5 were not dependent upon the total antibody dose; however, with increasing doses of ZME-018 there was a dose-dependent increase in  $t_{1/2}$  (from  $17.8 \pm 2$  h at the 2.5-mg dose to  $29 \pm 5$  h at the 20-mg dose). For 96.5 antibody, the apparent volume of distribution ( $V_d$ ) approximated the total blood volume ( $7.8 \pm 0.7$  l) at the 1-mg dose and decreased significantly at the 20-mg dose, suggesting saturation of extravascular antigen sites. In contrast, the  $V_d$  calculated for ZME-018 did not appear to be dependent upon the administered dose. Improved imaging occurred with increasing doses of unlabeled 96.5 above 2 mg, a finding not observed with ZME-018. The cumulative urine excretion of [ $^{111}\text{In}$ ] after administration of 96.5 or ZME-018 was 10%–14% of the total dose. These studies show that murine monoclonal antibodies of the same subtype but recognizing different surface antigens can exhibit markedly different *in vivo* pharmacokinetic behavior, which may partially explain differences in imaging noted with increasing doses of monoclonal antibody.

### Introduction

The availability of murine monoclonal antibodies reactive with a variety of tumor-associated antigens has stimulated considerable interest in their potential use for tumor imaging and therapy in man. Both animal models [1, 7, 8, 10, 16] and clinical trials [3, 4, 11, 17, 21] have clearly demonstrated that murine monoclonal antibodies can concentrate in human tumors with varying degrees of success.

Radiolabeled antibodies have been utilized by investigators to locate and visualize a variety of human tumors [12, 19]. There are several methods of radiolabeling proteins, one technique involving covalent binding of [ $^{111}\text{In}$ ] to antibodies with the functional chelating agent diethylenetriaminepenta-acetic acid (DTPA) [9]. Studies by Hagan et al. [5] have shown that antibodies labeled with [ $^{111}\text{In}$ ] appear to attain higher tumor-to-blood ratios than antibodies radiolabeled with iodine. This improvement appears to be related to the biological stability of the [ $^{111}\text{In}$ ] complex compared to that of the radio-iodinated protein. In addition, in contrast to the radio-iodination procedure, the binding affinity of the antibody is not substantially affected after [ $^{111}\text{In}$ ] labeling.

In concert with a phase I clinical trial to determine imaging effectiveness and toxicity, we studied the plasma pharmacokinetics and urinary excretion of the [ $^{111}\text{In}$ ]-labeled monoclonal antibodies 96.5 and ZME-018. Antibody 96.5 is reactive against the glycoprotein designated P97 found on most human melanoma cells [24, 25]. Antibody ZME-018 is reactive with epitope "a" of a 240-Kd surface glycoprotein (gp240) found on over 80% of melanoma cell lines and fresh tumor cells [23]. Both antibodies ZME-018 and 96.5 are of the IgG<sub>2</sub>A subclass.

The purpose of our study was to determine the pharmacokinetics of each antibody and to evaluate how changes in tissue distribution and tumor localization of labeled antibody reflect differences in antibody pharmacokinetics.

### Materials and methods

**Preparation of [ $^{111}\text{In}$ ]-labeled ZME-018 and 96.5.** The antibodies were produced as ascites in BALB/c mice as described previously [13, 25]. Both antibodies are of the IgG<sub>2</sub>A subclass. Antibodies ZME-028 and 96.5 were coupled to the chelating agent DTPA using a modification of the Krejarek technique [15]. The details of this method have been described elsewhere [10]. There was no apparent loss of antibody immunoreactivity by this method. The labeling yield was consistently 80%–100%, with routine specific activities being 10 mCi [ $^{111}\text{In}$ ]/mg antibody. Antibodies 96.5 and ZME-018 were supplied by Hybritech, Inc. in vials, already bound to DTPA. Immediately prior to use, the antibody was mixed with 2.5 or 5 mCi [ $^{111}\text{In}$ ] in aqueous HCl solution and appropriate neutralizing buffer.

**Patients.** Twenty-six patients with biopsy-proven malignant melanoma were selected for study of the 96.5 antibody. All patients gave written informed consent in accordance with guidelines established by the human subjects committee at M. D. Anderson Hospital and Tumor Institute. Patients in this study had not previously received murine antibodies. Each patient received either 1, 2, 5, 10, or 20 mg 96.5 antibody mixture comprised of 1 mg radiolabeled antibody and coupled to either 2.5 mCi (21 patients) or 5 mCi (5 patients) of [ $^{111}\text{In}$ ] and admixed with 1, 4, 9, or 19 mg of unlabeled antibody. There were 4 or 5 patients studied at each antibody dose level. For the ZME-018 antibody study, we selected another group of 25 patients with biopsy-proven malignant melanoma. In a similar manner, patients received 1 mg labeled antibody mixed with amounts of unlabeled antibody at concentrations of 2.5 mg (4 patients), 5 mg (5 patients), 10 mg (5 patients), 20 mg (6 patients), or 40 mg (5 patients). The antibody-isotope mixture was suspended in 200 ml normal saline and administered as a 2-h i. v. infusion delivered by infusion pump. Each patient received one infusion at a single dose level of antibody. Total-body imaging was performed using a longitudinal, tomographic imager (Phocon 192, Siemens Nuclear Imaging, Des Plaines, Ill) and multiple spot views were obtained using a larger field of view conventional gamma camera. In some cases, digital spot views were also acquired with computer-assisted data storage (Gamma 11-Digital Equipment Corporation, Westwood, Mass). Background subtraction techniques were not used. The results of toxicity and image analysis following administration of [ $^{111}\text{In}$ ]-labeled monoclonal antibodies, 96.5 and ZME-018, are presented elsewhere [17, 18]. To determine relative tissue distribution of the [ $^{111}\text{In}$ ] label, desitometric analyses were performed with an X-rite model 301 desitometer (X-Rite Company, Grand Rapids, MI 49508) on anterior and posterior scans obtained 4 h after infusion of labeled antibody.

**Method of comparing relative uptakes of [ $^{111}\text{In}$ ]-labeled monoclonal antibodies in tumor relative to background.** Region of interest scans (ROI) were drawn on the digital images taken at 72 hours post injection over the bones (lumbar spine), kidneys, and spleen. These were compared with ROIs over the liver and heart (blood pool) using average counts per pixel. When image collection was different from the standard 5 min, equalization was achieved first. If any visceral organ contained tumor, these were avoided in drawing ROIs.

**ELISA assay for murine monoclonal antibody in human serum.** In 96-well microtiter plates (Costar, Cambridge, Mass), a 50- $\mu\text{l}$  aliquot of 50 mM bicarbonate buffer (pH 9.6) containing 30  $\mu\text{g}$  goat anti-mouse IgG antibody (Cappel, Cochranville, Pa) per ml was added to each well. The plate was incubated overnight at room temperature and washed four times with 0.05% Triton X-100 using a 96-well plate washer (Dynatech, Santa Monica, Calif.). To each well, 50  $\mu\text{l}$  PBS containing 1% bovine serum albumin was added. In addition, 50  $\mu\text{l}$  of patient serum, PBS, or antibody standards in serum were diluted (1:2) with PBS and added to the plate in serial dilutions. The plates were incubated for 3 h at room temperature with shaking and then washed ten times with 0.05% Triton X-100. A 50  $\mu\text{l}$  aliquot of goat anti-mouse IgG conjugated to horseradish peroxidase (Cappel diluted 1:800) was added, and the plates

were further incubated for 2 hrs at room temperature with shaking. The plates were washed ten times with 0.05% Triton X-100. Then 200  $\mu\text{l}$  0.05 M phosphate: 0.025 M citrate buffer (pH 5.0) containing 0.4 mg *o*-phenylenediamine dihydrochloride (Sigma Chemical Co., St. Louis, Mo) per ml and 0.012%  $\text{H}_2\text{O}_2$  were added to each well. The plates were incubated in the dark for 30 min, and the reaction was stopped by the addition of 50  $\mu\text{l}$  2.5 M  $\text{H}_2\text{SO}_4$ . The plates were read at 490 nm in a Dynatech Model MR580 ELISA reader. Results from triplicate analysis of antibody standards were subjected to linear regression analysis for generation of standard curves. Values obtained from patient samples are the result of triplicate assays on dilutions within the dynamic range of the assay system.

**Radiological methods for [ $^{111}\text{In}$ ] measurement.** Whole blood samples (2 ml) were obtained from patients during [ $^{111}\text{In}$ ] infusion, at the end of the infusion (0), and at 1, 5, 10, 30, 60, 70, 120, 180, 1320 and 2760 min after the end of infusion. Blood samples were collected in 3-ml tubes containing sodium heparin anticoagulant. An aliquot (0.5 ml) of the [ $^{111}\text{In}$ ]-labeled antibody infusion solution was also obtained to serve as a standard and as an isotope decay control. Whole blood samples were centrifuged at 1500 rpm (Sorvall GLC-2B centrifuge), duplicate 100- $\mu\text{l}$  aliquots of plasma were added to glass 13- $\chi$  100-mm disposable test tubes. The tubes were loaded into plastic carriers, and [ $^{111}\text{In}$ ] activity was assessed using a Packard gamma scintillation spectrometer (Model 5360).

Urine samples were collected for 48 h following the infusion of antibody in 4- and 8-h aliquots. The total urine volume was measured, and duplicate 100- $\mu\text{l}$  aliquots were assayed for [ $^{111}\text{In}$ ] activity as described above. All analyses of [ $^{111}\text{In}$ ] activity were adjusted for isotopic decay. Values for [ $^{111}\text{In}$ ]-labeled antibody in plasma or values for murine antibody in plasma measured by ELISA assay were subjected to nonlinear regression analysis for calculation of standard pharmacokinetic parameters.

## Results

### Whole body images

The whole body tomographic images obtained from patients who received either antibody 96.5 or antibody ZME-018 at a dose of 20 mg are shown in Fig. 1 A and B, respectively. With antibody 96.5 there was substantial uptake, primarily in the liver. However, after administration of ZME-018 (Fig. 1 B), uptake of the radiolabel was observed primarily in spleen, kidney, bone, and testes.

### Plasma clearance curves for antibodies 96.5 and ZME-018

The plasma clearance curves for antibodies 96.5 and ZME-018 at a dose of 20 mg, 5 mCi [ $^{111}\text{In}$ ] are shown in Fig. 2. At this dose, the [ $^{111}\text{In}$ ]-label from both antibodies was cleared from plasma mono-exponentially and closely fit ( $r^2 > 0.9$ ) a one-compartment mathematical model. The calculated plasma half-lives at this dose were similar, at  $28 \pm 2$  h and  $29 \pm 5$  h for antibodies 96.5 and ZME, respectively.

### Pharmacokinetics of antibody 96.5

The pharmacokinetic summary for antibody 96.5 at doses between 1 and 20 mg is shown in Table 1. The plasma clearance for 96.5 antibody closely fit ( $r^2 > 0.9$ ) an open,

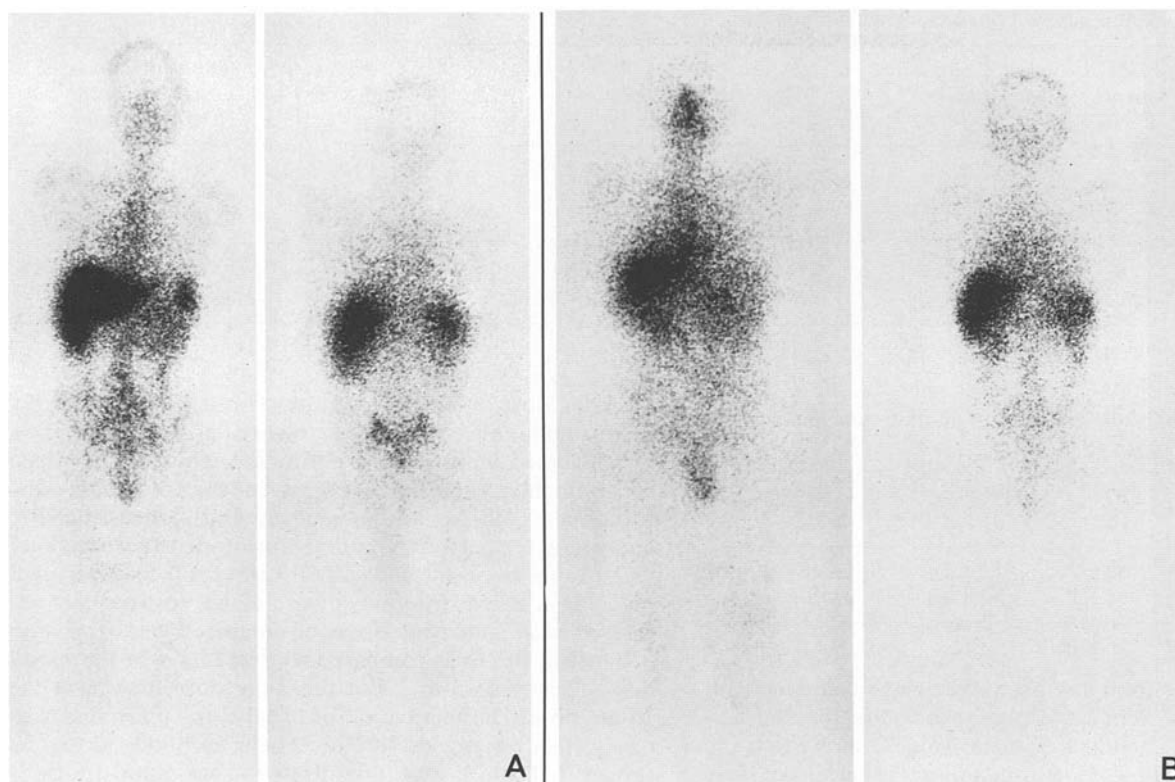


**Fig. 1 A.** Biodistribution of MoAb 96.5: anterior (*left*) and posterior (*right*) views of total-body tomograms taken at 72-h are shown. Note intense liver uptake with considerable activity in blood pool. **B** Biodistribution of MoAb ZME-018. Views as above. Note lesser uptake in liver (compared with 96.5 antibody) with more radioactivity in spleen and kidneys. There also appears to be some residual activity in the pelvis and spine along with the testes and nasopharynx

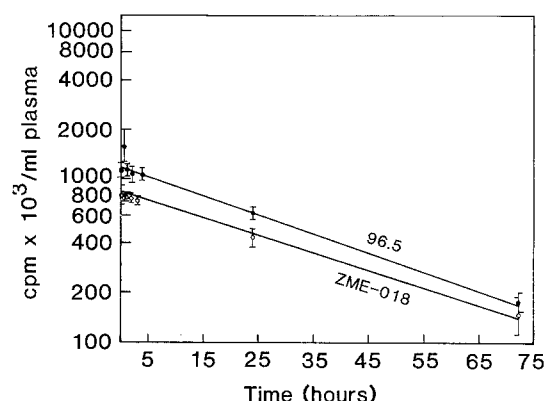


**Fig. 2.** Clearance of murine monoclonal antibody 96.5 and ZME-018 from plasma. The *open circles* show the clearance of the [<sup>111</sup>In] label from plasma in 7 patients who received 20 mg 96.5 antibody at a dose of 5 mCi [<sup>111</sup>In]. *Closed circles* show the clearance of murine monoclonal antibody ZME-018 from plasma of patients who received 20 mg antibody at a dose of 5 mCi of [<sup>111</sup>In]. The *solid lines* show the best-fit, least-squares regression lines through these points. Values shown are mean  $\pm$  SEM

one-compartment mathematical model. This was found to be the case regardless of antibody dose, size of tumor burden in the patient, or degree or extent of labeled antibody uptake of the tumor. The plasma half-life calculated for 96.5 was  $27 \pm 9$  h at the 1-mg dose and did not appear to vary with the dose of either unlabeled antibody or the

dose of [<sup>111</sup>In] administered. However, the apparent volume of distribution ( $V_d$ ) of the [<sup>111</sup>In]-labeled antibody was found to be significantly lower at the 5-mg dose than at the 2-mg dose level (Table 1). At doses of 96.5 higher than 5 mg, the apparent volume of did not appear to change substantially. Similarly, the 48-h cumulative urinary excretion of the [<sup>111</sup>In] label varied from  $23\% \pm 6\%$  to  $12\% \pm 5\%$  of the total dose administered and did not appear to be dependent on the dose of antibody.

The clearance of murine monoclonal antibody from plasma was measured by ELISA assay. The clearance of monoclonal antibody from plasma exactly paralleled the clearance of the [<sup>111</sup>In] label as shown in Fig. 2. In addition, the pharmacokinetic parameters calculated from nonlinear regression analysis of murine antibody clearance from plasma (Table 2) were identical to the pharmacokinetic parameters calculated from measurement of the [<sup>111</sup>In] clearance from plasma. These data suggest that the [<sup>111</sup>In] label remains attached to the antibody after *in vivo* administration.

#### *Pharmacokinetics of antibody ZME-018*

In contrast to the invariant, one-phase clearance found for antibody 96.5, the disappearance for antibody ZME-018 from plasma closely fit a one-compartment model for clearance in some patients and a two-compartment model in others (Table 2). Biphasic clearance profiles were found in 2 of 4 patients at the 2.5-mg dose level and in 2 of 5 patients at the 10-mg dose level. There were no differences

**Table 1.** Monoclonal antibody 96.5 pharmacokinetic summary<sup>a</sup>

Antibody dose (mg)	No. of patients	[ <sup>111</sup> In] dose (mCi)	t <sub>1/2</sub> (h)	V <sub>d</sub>	C × t (μCi/ml × h)	48-h cumulative urinary excretion (% of total dose)
1	4	2.5	27 ± 9	7.8 ± 0.7	357 ± 127	23 ± 6
2	5	2.5	36 ± 3	7.5 ± 0.6	428 ± 47	19 ± 3
5	5	2.5	32 ± 3.4	4 ± 0.3	642 ± 45	18 ± 2
10	5	2.5	31 ± 4	4 ± 0.8	653 ± 106	17 ± 4
20	2	2.5	39 ± 9	4.4 ± 0.1	1081 ± 296	12 ± 5
20	5	5.0	28 ± 2	3.0 ± 0.09	1486 ± 126	16 ± 2

<sup>a</sup> Values shown are means ± SEM**Table 2.** Pharmacokinetic summary of murine monoclonal antibody

Dose (mg)	No. of patients	t <sub>1/2</sub> (h)	V <sub>d</sub> (l)	C × t (μ/ml × min)
2	3	32 ± 2	3.5 ± 2	72 ± 3
20	9	31 ± 3	3.1 ± 0.3	321 ± 49

between the patients at any dose level which could account for these effects. While the plasma half-life for 96.5 appeared to be independent of dose, Table 2 shows that the plasma half-life for ZME-018 demonstrates clear-cut dose dependence, increasing from 17.8 ± 2.13 h at the 2.5-mg dose to 33.6 ± 3 h at the 40 mg dose level. The apparent volume of distribution for ZME-018 was 4.6 ± 0.7 l at the 2.5-mg dose and did not appear to vary with the dose of antibody administered.

Patients who received ZME-018 at the 10- and 20-mg doses (11 patients) demonstrated a wide variation in the calculated plasma half-life. The group included 8 patients with a relatively large tumor burden (> 10 cm<sup>2</sup>, Table 3) and 3 patients with a relatively small total tumor burden (< 10 cm<sup>2</sup>).

As shown in Table 3, in the patient group with a tumor large burden the plasma half-life was significantly shorter (by 50%; *P* < 0.001) than in patients with a relatively small tumor mass. There was no correlation of tumor mass with plasma half-life at other dose levels of ZME-018, nor was there a similar correlation for antibody 96.5 at the doses studied. It is, therefore, unclear whether this was a result of a dose-related effect confined to this particular antibody.

#### Tissue distribution of antibody 96.5 and ZME-018

The greatest decrease in the apparent volume of distribution with antibody 96.5 (Table 1) was observed between

the 2-mg dose and the 5-mg dose. This appears to sharply define a boundary point for extravascular tissue saturation by unlabeled antibody. To define the major tissue site(s) which might account for this apparent change in tissue distribution of labeled antibody, comparative densitometric analyses were performed after infusion of either antibody 96.5 (Table 4) or antibody ZME-018 (Table 5). As shown in Table 4, the distribution of radiolabel to liver was decreased with increasing doses of unlabeled 96.5. The ratio of label in the liver compared to that found in the blood pool decreased from 2.7 at the 2-mg dose to 0.88 at the 20-mg dose. The relative ratios of label in spleen and kidney were unchanged with increasing antibody dose. As shown in Table 6, and in contrast to that found for 96.5,

**Table 4.** Plasma half-life of ZME-018 related to total tumor burden

Total tumor burden (cm <sup>2</sup> )	Patient No.	Plasma t <sub>1/2</sub> (min)
> 10	1	987
	2	1462
	3	1639
	4	2026
	5	888
	6	1408
	7	1490
	8	1074
$\bar{X} \pm \text{SEM}$		1372 ± 133
< 10	9	2748
	10	2163
	11	2844
$\bar{X} \pm \text{SEM}$		2585 ± 213*

\* *P* < 0.001**Table 3.** ZME-018 pharmacokinetic summary

Antibody dose (mg)	No. of patients	[ <sup>111</sup> In] dose (μCi)	t <sub>1/2</sub> (h)		V <sub>d</sub> (l)	C × t (μCi/ml × h)	48-h cumulative urinary excretion (% of total dose)
			α	β			
2.5	4	5	1.46 ± 0.33	17.8 ± 2.13	4.6 ± 0.7	483 ± 72.2	16.7 ± 5.4
5.0	5	5		24.5 ± 2.7	4.0 ± 0.5	752 ± 133.3	8.7 ± 0.5
10.0	5	5	3.3 ± 3.1	27.5 ± 5	3.6 ± 0.5	929 ± 217.6	9.6 ± 0.8
20.0	6	5		29.1 ± 5	4.4 ± 0.4	943 ± 196	10.5 ± 1.7
40.0	5	5		33.6 ± 3.7	3.84 ± 0.55	1119.46 ± 211.99	11.72 ± 2.19

<sup>a</sup> Values shown are means ± SEM

the distribution of ZME-018 to liver did not appreciably change with increasing dose of unlabeled antibody. In addition, the concentration of labeled ZME-018 in spleen and kidney was found to decrease significantly with increasing antibody doses, again, in contrast to the tissue distribution behavior described for antibody 96.5.

#### *Comparative imaging effectiveness of antibody 96.5 and ZME-018*

The number of known metastatic lesions imaged at various doses of antibody 96.5 is shown in Table 7. With increasing dose of antibody and decreasing specific activity of the [ $^{111}\text{In}$ ] label, there was a substantial increase in the percen-

tage of known tumor sites imaged. The greatest imaging occurred at 20 mg antibody with 5 mCi of [ $^{111}\text{In}$ ] label. There were also two sites of antibody uptake into soft tissue which were not previously identified as tumor sites. Because of the position of the sites, a biopsy to either confirm or rule out the presence of tumor could not be performed.

The imaging effectiveness of various doses of ZME-018 is shown in Table 8. With increasing antibody dose from 1 mg to 5 mg, imaging effectiveness increased from 25% to 60%, respectively. However, at doses above 5 mg and, therefore, decreasing specific activity, imaging effectiveness remained between 60% and 74% of known sites imaged. In addition, the number of uncorrelated sites of isotope uptake increased at higher antibody doses.

**Table 5.** Tissue distribution<sup>a</sup> of [ $^{111}\text{In}$ ] monoclonal antibody 96.5

Dose (mg)	No. of patients	Tissue ratios		
		S/H	L/H	K/A
2	5	0.56	2.7	1.76
5	5	0.54	1.30	1.60
10	5	0.54	1.16	1.36
20	4	0.50	0.88	1.30

H, heart; S, spleen; L, liver; K, kidney; A, aorta

<sup>a</sup> Relative tissue concentrations measured by densitometer analysis of whole-body scans obtained 4 h after infusion end. Values shown are means of those obtained from both anterior and posterior scans of four or five patients at each dose level

**Table 6.** Tissue distribution of [ $^{111}\text{In}$ ] monoclonal antibody ZME-018

Dose (mg)	No. of patients	Tissue ratios		
		S/H	L/H	K/H
2.5	5	4.17 $\pm$ 0.92	2.08 $\pm$ 0.15	1.65 $\pm$ 0.25
5	5	3.82 $\pm$ 0.80	2.90 $\pm$ 0.42	1.57 $\pm$ 0.19
10	5	2.17 $\pm$ 0.10	2.03 $\pm$ 0.20	1.13 $\pm$ 0.14
20	5	1.83 $\pm$ 0.18	2.20 $\pm$ 0.50	0.97 $\pm$ 0.07

H, heart or blood pool; L, liver; K, kidney; S, spleen;

<sup>a</sup> Relative tissue concentrations measured by online analysis of the digital image of the region of interest (ROI) scans obtained 72 h after infusion end

**Table 7.** Number of metastases imaged in relation to dose of MOAB 96.5

Dose of MOAB (mg/patient)	Mean dose [ $^{111}\text{In}$ ] (mCi)	Mean sp. act. [ $^{111}\text{In}$ ] (mCi/mg)	No. of patients studied	Metastases <sup>a</sup>		Number of uncorrelated sites of isotope uptake <sup>b</sup>
				Known	Imaged (%)	
1	2.3	2.3	4	23	2 (9)	0
2	2.3	1.2	5	10	5 (50)	0
5	2.2	0.44	5	10	4 (40)	0
10	2.3	0.23	5	12	9 (75)	0
20	2.5	0.13	3	43	15 (35)	0
20	5.0	0.25	8	31	25 (81)	2
Total			31	130	61 (47)	2

<sup>a</sup> In three patients, two at 1 mg, one at 2 mg, metastases were too small and too numerous to count accurately. These were recorded by site rather than number

<sup>b</sup> Indicates uptake of tracer in areas (excluding liver spleen and bone marrow) not previously identified as metastases

**Table 8.** Number of metastases imaged in relation to dose of MOAB ZME-018

Dose MOAB (mg)	Mean sp. act. [ $^{111}\text{In}$ ] (mCi/mg)	Patients studied	Metastases <sup>a</sup>		Number of uncorrelated sites of isotope uptake <sup>b</sup>
			Known	Imaged (%)	
2.5	2.0	4	24	7 (29)	0
5	1.0	5	10	6 (60)	3
10	0.50	5	17	11 (65)	0
20	0.25	6	42	31 (74)	6
Total		21	97	56 (58)	9

## Discussion

Although murine monoclonal antibodies have the potential to localize within human tumors, there are a variety of factors which may influence antibody acquisition by tumors *in vivo* [1]. Some of these factors are tumor-dependent, and they include: cell heterogeneity of surface antigen expression, tumor size, and blood flow to the tumor [21]. Other factors which can affect *in vivo* antibody localization within tumors are dependent on the characteristics of the surface antigen and the particular antibody [22, 23].

The pharmacokinetic handling of murine monoclonal antibodies are probably affected by an interplay of tumor-dependent, antibody-dependent, and antigen-dependent factors, all of which can influence antibody clearance from the plasma, tumor localization, and metabolism. It is therefore not surprising that this study demonstrated that murine antimelanoma antibodies of the same immunoglobulin subclass but recognizing different cell surface antigens have substantially different pharmacokinetic behavior. Furthermore, the two monoclonal antibodies examined also exhibit markedly different patterns of tissue distribution and tumor localization with increasing dose of antibody.

One possible explanation for the observed differences in pharmacokinetics between these two antibodies may be the fact that each antibody cross-reacts to a greater or lesser extent with non-target tissues. The antigen recognized by antibody 96.5 designated P97 has structural homology with transferrin [24]. Therefore, the binding of antibody 96.5 in some non-target tissues may be due to its transferrin cross-reactivity. Unlike antibody 96.5, ZME-018 reacts against a high-molecular-weight glycoprotein (gp240) and does not cross-react with transferrin. Therefore, the whole-body distribution and pharmacokinetics of each antibody may vary depending on antibody specificity.

Particularly surprising was the finding that the plasma half-life of ZME-018 at the 10- and 20-mg dose levels appeared to be dependent on the total size of the patient's tumor (Table 3). Since tumor should (ideally) represent a major compartment for antibody clearance, the plasma half-life of the antibody in patients with a large tumor burden should be different from that in patients with a smaller tumor mass. It is not clear why this phenomena was not observed in patients after administration of antibody 96.5.

Various clinical studies of labeled monoclonal antibodies have incorporated pharmacokinetic analysis [6, 21, 24, 25]. The pharmacology of murine monoclonal antibodies appears to be unique for each antibody studied. Similarly, the clinical imaging effectiveness of monoclonal antibodies also appears to be unique for each antibody studied. Therefore, it may not be possible to make generalizations concerning the behavior of new antibodies based on prior studies of other antibodies.

## References

- Bourdon MA, Coleman RE, Blasberg RG, Brothuis DR, Bigner DD (1984) Monoclonal antibody localization in subcutaneous and intracranial human glioma xenografts: paired-label and imaging analysis. *Anticancer Res* 4: 133–140
- Brown JP, Hewick RM, Hellstrom I, Hellstrom KE, Doolittle RF, Dreyer WJ (1982) Human melanoma-associated antigen P97 is structurally and functionally related to transferrin. *Nature* 296: 171–173
- Goldenberg DM, Kim EF, DeLand FH, van Nagell JR, Javdipour N (1980) Clinical radioimmunodetection of cancer with radioactive antibodies to human chorionic gonadotropin. *Science* 208: 1284–1286
- Goldenberg DM, Kim EF, DeLand FH, Spremulli E, Nelson MO, Gockerman JP, Primus FJ, Corgan RL, Alpert E (1980) Clinical studies on the radioimmunodetection of tumors containing alpha fetoprotein. *Cancer* 45: 2500–2505
- Hagan PL, Halpern SE, Chen Awn, Frincke JM, Bartholomew RM, David GS, Carlo DJ (1983) Comparison of  $^{111}\text{In}$ -labeled Fab and whole  $^{111}\text{In}$  anti-CEA monoclonal antibody (MoAb) in normal mouse and human colon tumor models. *J Nucl Med* 24: 77
- Halpern SE, Hagan P (1985) Effect of protein mass on the pharmacokinetics of murine monoclonal antibodies. *J Nucl Med* 26: 818–819
- Halpern SE, Stern PH, Hagan PL, Chen Awn, David GS, Desmond WJ, Adams TH, Bartholomew RM, Frincke JM, Brautigam CE (1981) Radiolabeling of monoclonal tumor antibodies, comparison of I-125 and In-111 anti-CEA with GA-67 in a nude mouse-human colon tumor model. *Clin Nucl Med* 6: 453
- Halpern SE, Hagan PL, Garver PR, Bartholomew RM, Frincke JM, McEvoy S, Adams TH (1982) Comparison of In-111 anti-CEA monoclonal antibodies (MoAb) and endogenously labeled Se-75 MoAbs in normal and tumor bearing mice. *J Nucl Med* 23: 8
- Halpern SE, Hagan PL, Garver PR, Bartholomew RM, Frincke JM, McEvoy S, Adams TH (1982) Comparison of In-111 anti-CEA monoclonal antibodies (MoAb) and endogenously labeled Se-75 MoAbs in normal and tumor-bearing mice. *J Nucl Med* 23: 18
- Halpern SE, Stern PH, Hagan PL, Chen Awn, Frincke JM, Bartholomew RM, David GS, Adams TH (1983) Stability characterization and kinetics of  $^{111}\text{In}$ -labeled monoclonal anti-tumor antibodies in normal animals and nude mouse-human tumor models. *Cancer Res* 43: 5347–5355
- Halpern SE, Dillman RO, Hagan PL, Dillman JD, Royston I, Sobol RE, Frincke JM, Bartholomew RM, David GS, Carlo DJ (1983) The clinical evaluation of  $^{111}\text{In}$ -labeled monoclonal anti-melanoma antibodies ( $^{111}\text{In}$  anti-mel) for human scanning. *J Nucl Med* 24: 15
- Hayes DF, Zalutsky MR, Kaplan W, Noska M, Thor A, Colcher D, Kufe DW (1986) Pharmacokinetics of radiolabelled monoclonal antibody B6.2 in patients with metastatic breast cancer. *Cancer Res* 46: 3157–3163
- Hellstrom I, Brown JP, Hellstrom KE (1981) Monoclonal antibodies to two determinants of melanoma-antigen P97 act synergistically in complement dependent cytotoxicity. *J Immunol* 127: 157–160
- Hnatowich DJ, Griffin TW, Kosciwicz C, Rusckowski M, Childs RL, Mattis JA, Shealy P, Doherty PW (1985) Pharmacokinetics of an  $^{111}\text{In}$ -labeled monoclonal antibody in cancer patients. *J Nucl Med* 26: 849–858
- Krejcarek CE, Tucker KL (1977) Covalent attachment of chelating groups to macromolecules. *Biochem Biophys Res Commun* 177: 581–585
- Moshakis V, Bailey MJ, Ormerod MG, Westwood JH, Neville AM (1981) Localization of human breast carcinoma xenografts using antibodies to carcinoma-embryonic antigen. *Br J Cancer* 43: 575–581
- Murray JL, Rosenblum MG, Sobol RE, Bartholomew RM, Plager CE, Haynie TP, Jahns MF, Glenn HJ, Benjamin RS, Papadopoulos N, Boddie AW, Frincke JF, David GS, Carlo DJ, Hersch EM (1985) Radioimmunodetection in malignant melanoma with  $^{111}\text{In}$ -labeled monoclonal antibody 96.5. *Cancer Res* 45: 2376–2381
- Murray JL, Rosenblum MG, Lamki L, Haynie TP, Glenn HJ, Plager CE, Unger MW, Carlo DJ, Hersch EM (1987) Radioimmunodetection in malignant melanoma patients using  $^{111}\text{In}$ -

- labeled anti-melanoma monoclonal antibody (ZME-018) to a high M. W. antigen Kd 240. NCI Monographs (in press)
19. Oldham RK, Foon KA, Morgan AC, Woodhouse CS, Schroff RW, Abrams PG, Fer M, Schoenberger CS, Farrell M, Kimball E, Sherwin SA (1984) Monoclonal antibody therapy of malignant melanoma: in vivo localization in cutaneous metastasis after intravenous administration. *J Clin Oncol* 2: 1235–1244
  20. Rosenblum MG, Murray JL, Haynie TP, Glenn HJ, Jahns MF, Benjamin RS, Frincke JM, Carlo DJ, Hersh EM (1985) Pharmacokinetics of <sup>111</sup>In-labeled anti-P97 monoclonal antibody in patients with metastatic malignant melanoma. *Cancer Res* 45: 2382–2386
  21. Sullivan DC, Silva JS, Cox CE, Haagensen DE Jr, Harris CC, Briner WH, Wells SA Jr (1987) Localization of i-131 labeled goat and primate anti-carcino-embryonic antigen (CEA) antibodies in patients with cancer. *Invest Radiol* 17: 350–355
  22. Weinstein JN, Steller MA, Covell DG, Holton OD, Keenan AM, Sieber SM, Parker RJ (1984) Monoclonal antitumor antibodies in the lymphatics. *Cancer Treat Rep* 68: 257–264
  23. Wilson BS, Imai K, Natali AG, Ferrone S (1981) Distribution and molecular characterization of a cell-surface and a cytoplasmic antigen detectable in human melanoma cells with monoclonal antibodies. *Int J Cancer* 28: 293–300
  24. Woodbury RG, Brown JP, Loop SM, Hellstrom KE, Hellstrom I (1981) Analysis of normal neoplastic human tissues for the tumor-associated protein P97. *Int J Cancer* 27: 145–149
  25. Woodbury RG, Brown JP, Yeh MY, Hellstrom I, Hellstrom KE (1980) Identification of a cell surface protein, P97, in human melanomas and certain other neoplasms. *Proc Natl Acad Sci, USA* 77: 2183–2186

Received August 5, 1985/Accepted April 3, 1987